arXiv:1504.01213v3 [hep-ph] 11 Apr 2016

Anapole moment of the lightest neutralino in the cMSSM

Luis G. Cabral-Rosetti[a], Myriam Mondragón[b], Esteban Reyes-Pérez[b]

[a]Centro Interdisciplinario de Investigación y Docencia en Educación Técnica, CIIDET. Av. Universidad 282 Pte., Col. Centro, A. Postal 752, C.P. 76000, Santiago de Querétaro, Qro., México.

cabralrosetti@gmail.com

[b] Instituto de Física, Universidad Nacional Autónoma de México Apdo. Postal 20-364, C.P. 01000, Ciudad de México, México.

myriam@fisica.unam.mx esteban.reyesperez@gmail.com

Abstract

We study the anapole moment of the lightest neutralino in the constrained Minimal Supersymmetric Standard Model (cMSSM). The electromagnetic anapole is the only allowed electromagnetic form factor for Majorana fermions, such as the neutralino. Since the neutralino is the LSP in many versions of the MSSM and therefore a candidate for dark matter, its characterization through its electromagnetic properties is important both for particle physics and for cosmology. We perform a scan in the parameter space of the cMSSM and find that the anapole moment is different from zero albeit very small ($< 10^{-3}$ GeV^{-2}). Combined with experimental constraints like the Higgs mass and the DM relic density, the allowed region of parameter space lies within the reach of future direct DM searches. Thus, the anapole moment could be used as a complementary constraint when studying the parameter space of the cMSSM and other similar models.

1 Introduction

One of the best motivated extensions of the Standard Model (SM) is the Minimal Supersymmetric Standard Model (MSSM), since, besides giving a solution to the hierarchy problem, it provides us with a good candidate for cold dark matter (CDM), namely, the lightest neutralino.

A number of different experiments are working (or will be soon) in the search for a direct or an indirect signal of dark matter (DM) (for recent reviews on dark matter detection see [1, 2]). If DM is detected, there will be a need to differentiate between the candidates, characterizing them as much as possible. In the last few years, there has been intense work on the electroweak properties of dark matter since they might be relevant for the calculation of DM decays and annihilations, [3–15], which have consequences in astrophysical processes [16, 17] and are important in indirect astrophysical searches for DM, as in the calculation of the annihilation cross section of the DM itself.

Motivated by this, since 2009 we have been studying the toroidal dipole moment (TDM) of Majorana particles, which is related to the anapole moment, one of the least studied electromagnetic properties of a particle [18–21]. Lately, there has been a surge of interest in the study of anapole moments from the astrophysical as well as the particle physics points of view (e.g. [22–25]).

Since first discussed in 1957, the anapole moment, introduced by Zel'dovich [26], has been investigated in different fields of science and technology. The anapole moment corresponds to a T invariant interaction, which is C and P non-invariant [26]. Within the Standard Model it has been calculated in neutrino and hadron physics [27–30]. In nuclear physics it has been studied in atomic nuclei [31–33]. In relation to the DM problem, there are different proposals to observe this "physical observable", extracting its value from direct measurements between DM and atomic nuclei [23, 24, 34, 35]. Finally, in engineering various aplications have been studied, in areas such as "Ferrite resonators" [36], electromagnetic properties in dielectric nanoparticles [37], and in the study of electromagnetic radiation in antennae with a helicoidal toroidal geometric distribution [38–42], among others.

Recently, Ho and Scherrer have proposed that dark matter interacts with ordinary matter exclusively through the anapole moment [22]. They calculate the anapole moment needed to obtain the right amount of DM relic abundance, and the anapole DM signatures that could be observed in the LHC [43]. Haish and Kahlhoefer have shown the importance of loop contributions to the scattering cross section of dark matter, in particular those induced by the anapole interaction [44]. More recently, del Nobile et al made a halo-independent analysis of direct DM detection data considering that it has only anapole and magnetic moment dipole interactions [24]. Also, an analysis on the loop corrections for leptophilic DM and internal bremsstrahlung was

presented in [23], where the authors calculate the DM anapole and dipole moments in a toy model using direct detection data.

In this paper we calculate the anapole moment of the neutralino at the one-loop level within the constrained Minimal Supersymmetric Standard Model (cMSSM). In the MSSM the anapole contributions of the neutralino arise exclusively through radiative corrections to the vertex $\chi\bar{\chi}\gamma$. We do a scan in the five parameter space of the cMSSM and compare the results for the anapole moment with the above mentioned experimental limit. In our analysis we take into account also other experimental constraints, namely the Higgs boson mass and the decays $b \to s\gamma$ and $B \to \mu^+\mu^-$ in order to find the viable regions of parameter space. We find that although the anapole moment is very small througout the regions studied, it is possible to distinguish between the different regions of parameter space through it, which makes it indeed an important property when characterising dark matter. Our results agree qualitatively with those found by Ho and Scherrer [22].

The article is organised as follows: in section II we present a very brief summary of some aspects of the constrained MSSM relevant to our calculation. In section III we review the general form for the electromagnetic vertex of a particle, and in particular for a Majorana particle. We introduce the anapole moment and its relation to the toroidal dipole moment. In section IV we explain the methodology used to calculate the anapole moment of the neutralino in the cMSSM and evaluate it for different values of the parameters. Section V presents the obtained results and our conclusions.

2 The MSSM and the neutralino as candidate for dark matter

According to the latest results of WMAP, the CDM density is [45]

$$\Omega_{DM}h^2 \sim 0.1109 \ , \tag{1}$$

where h is the Hubble constant in units of 100 km sec^{-1} Mpc^{-1}. The thermally averaged effective cross section times the relative speed of the dark matter particle, needed to get this relic density is [46–48]

$$< \sigma v > \propto g^4_{weak}/16\pi^2 m_x^2 \tag{2}$$

consistent with the assumption of a weakly interacting dark matter particle (WIMP) with a mass between 10 GeV - (few) TeV.

The minimal supersymmetric extension of the Standard Model (MSSM) provides us with one of the best WIMP candidates for dark matter: the lightest neutralino (for reviews on SUSY see for instance [49, 50]). The MSSM requires two complex Higgs electroweak doublets to give mass to the up and down type quarks in order to avoid chiral anomalies. The MSSM has also a new discrete symmetry, R parity, defined as $R = (-1)^{3B+2S+L}$, where B and L are the baryonic and leptonic numbers respectively. This symmetry assignes a charge +1 to the SM particles and -1 to the supersymmetric partners, making the lightest supersymmetric particle (LSP) stable.

However, supersymmetry has to be broken or it would have already been observed. To break it explicitly without the reappearance of quadratic divergencies, a set of super-renormalizable terms are added to the Lagrangian, the so-called soft breaking terms. The Lagrangian for the soft breaking terms is given by

$$\mathcal{L}_{soft} = -\frac{1}{2}M_a\lambda^a\lambda^a - \frac{1}{6}A^{ijk}\phi_i\Phi_j\phi_k - \frac{1}{2}B^{ij}\phi_i\phi_j + c.c. - (m^2)^i_j\phi^{j*}\phi_i \ , \quad (3)$$

where M_a are the gaugino masses, A^{ijk} and B^{ij} are trilinear and bilinear couplings respectively, and $(m^2)^i_j$ are scalar squared-mass terms. It is assumed that supersymmetry breaking happens in a hidden sector, which communicates to the observable one only through gravitational interactions, and that the gauge interactions unifiy. This means that at the GUT scale the soft breaking terms are "universal", i.e., the gauginos M_a have a common mass, as well as the scalars $(m^2)^i_j$ and the trilinear couplings, A^{ijk}. Requiring electroweak symmetry breaking fixes the value of B^{ij} and the absolute value of the Higgsino mixing parameter $|\mu|$. This is known as the constrained MSSM (cMSSM) which is described by five parameters: the unified gaugino mass $m_{1/2}$, the universal scalar mass m_0, the value of the universal trilinear coupling A_0, the sign of Higgsino mass parameter μ, and the ratio of the vacuum expectation values of the two Higgses, $\tan\beta$.

After the electroweak symmetry breaking the neutral and charged states in the MSSM can mix. In the case of the neutral ones they give rise to a set of four mass eigenstates, the neutralinos. It is the lightest one of these that is the LSP and a good candidate to dark matter in many SUSY models. The lightest neutralino, in the gauge eigenstate basis, is a function of the neutral higgsinos and the neutral gauginos (wino and bino) and its properties will depend on the mixing, which in turn depends on the soft breaking parameters.

Before WMAP, the cMSSM was compatible with the limit $\Omega_{DM,0}h^2 \sim 0.1 - 0.3$ and other direct and indirect low energy and collider data in a huge parameter space region called the "bulk". However, after the constraint by WMAP to $\Omega_{DM,0}h^2$, and with the recent limits to the sparticles masses from the LHC, which excludes light masses, the bulk region in $m_0 - m_{1/2}$ is no longer viable. Moreover, in the cMSSM the LSP neutralino is, practically for all cases, an almost pure bino state which annihilates itself more efficiently into leptons through right hand sleptons due to their higher hypercharge. However, with the newest data from WMAP, this mechanism is not sufficiently efficient. There are still three favoured scenarios that require some very specific accidental relations between some parameters at the electroweak scale.

In the cMSSM at low m_0, there is a region with almost degenerate $\tilde{\tau} - \tilde{\chi}_1^0$. In this case the populations of these two particles are almost the same, making the NLSP $\tilde{\tau}$ thermally accesible. The mass diference between the scalar tau and the lighest neutralino, $\Delta M = m_{\tilde{\tau}} - m_{\tilde{\chi}_1^0}$, controls the population ratio of these two species through the Boltzmann factor $\exp(-\Delta M/T_f)$. Therefore, it is a very sensitive parameter which enters into the calculation of the relic density. Whenever the coannihilation takes place, through the participation of $\tilde{\tau}$ in processes like $\tilde{\tau}_1\tilde{\chi}_1^0 \longrightarrow \tau\gamma$ or even $\tilde{\tau}_1\tilde{\tau}_1 \longrightarrow \tau\tilde{\tau}$, the relic density can be reduced in comparison to the case of the bulk scenario. In this region, the LSP neutralino is mainly bino with a mass esentially stablished by M_1 up to corrections of order M_Z^2/μ (μ is high). The approximate formulae for the mass of the neutralino and the mass of $\tilde{\tau}_1$ suggest that degeneration happens for $m_0 \sim 0.145\ m_{1/2}$.

A sudden increase in the usual mechanism of coannihilation to reduce the relic density can occur if $m_{\tilde{\chi}_1^0}$ is close to a pole. Faster and more efficient annihilation can take place through Higgs resonance. Given the Majorana nature of the neutralino, the resonant *enhancement* is obtained only via the pseudo-scalar Higgs boson. The colliders constrains to the LSP in the cMSSM allow the heavy "Higgs funnel", where $\tilde{\chi}_1^0\tilde{\chi}_1^0 \longrightarrow A \longrightarrow b\bar{b}/\tau\bar{\tau}$, which happens for high $\tan\beta$. Therefore, the quantities that establish this scenario are the quantity $2m_{\tilde{\chi}_1^0} - m_A$ and the amplitude of the pseudo-scalar, since they define the resonance profile of A.

In most of the cMSSM, μ is very high. However, you can exceptionally have that $\mu \sim M_1$, which allows much more efficient coannihilation through reactions as $\tilde{\chi}_1^0\tilde{\chi}_1^0 \longrightarrow WW/ZZ/Zh/t\bar{t}$. This happens in the so-called focus point region where m_0 is very high. The focus point region corresponds

to high values of m_0 close to the border of viable electroweak symmetry breaking, where the value of μ decreases rapidly. When $\mu \sim M_1$, M_2, the LSP has a significant fraction of higgsino, and the next lightest sparticles ($\tilde{\chi}_2^0$ o $\tilde{\chi}_1^{\pm}$) have also a significant component of higgsino and are not much heavier than the LSP. Thus, the coannihilation channels are favoured. However, coannihilation cannot be very efficient, otherwise the relic density would be less than what is actually measured. In this scenario, all the sfermions are very heavy (more than 4 TeV) to be accesible to one of the proposed colliders. The LSP mass goes from close to 150 to 350 GeV, with higgsino-type neutralinos being 100 to 50 GeV heavier. From the perspective of a linear collider, an energy of more than 800 GeV is needed to reveal some of the properties of this scenario. The pseudo-scalar has a mass higher than 1 TeV and very likely would not be found directly in the LHC.

There have been several scans of the cMSSM and other MSSM type models using different criteria to check its viability. Many of these are either Bayesian (e.g. [51–55]) or frequentist (e.g. [56–58]), or both ([59, 60]), but there are also many studies using other techniques or constraints to perform the analysis (e.g. [61–65]). In the cMSSM it is assumed that DM is composed by only one type of particle, the LSP, which is usually assumed to be the neutralino. Most of the studies then look for regions of likelihood with different boundary conditions at the GUT scale, i.e. values for $m_0, m_{1/2}, \tan\beta, \mu$ and A_0, and phenomenological constraints at low energies, which usually include a combination of the following: the branching ratios $b \to s\gamma$, $B \to \mu^+\mu^-$, the dark matter relic density, the requirement of radiative electroweak symmetry breaking, the Higgs mass, and a solution to the $g-2$ problem (although not all of these constraints may be considered together in every analysis), and constraints coming from direct and indirect searches for dark matter. From these various scans it is clear that the cMSSM is highly challenged, although there are still regions of parameter space allowed, depending on which low energy constraints are used. In general, to satisfy most of the above constraints, a heavy supersymmetric spectrum is expected, with $A_0 \neq 0$ and large $\tan\beta$ (for a recent overview on constraints on the cMSSM and other SUSY models see for instance [56, 58, 66, 67]).

3 Anapole Moment

For 1/2-spin particles the most general expression for the electromagnetic vertex function, which characterizes the interaction between the particle and the electromagnetic field, is:

$$\Gamma_\mu(q) = f_Q(q^2)\gamma_\mu + f_\mu(q^2)i\sigma_{\mu\nu}q^\nu\gamma_5 \\ -f_E(q^2)\sigma_{\mu\nu}q^\nu + f_A(q^2)(q^2\gamma_\mu - \not{q}q_\mu)\gamma_5, \tag{4}$$

where $f_Q(q^2)$, $f_\mu(q^2)$, $f_E(q^2)$ and $f_A(q^2)$ are the so called charge, magnetic dipole, electric dipole and anapole form factors, respectively; in here $q_\mu = p'_\mu - p_\mu$ is the transferred 4-momentum and $\sigma_{\mu\nu} = (i/2)\left[\gamma_\mu, \gamma_\nu\right]$ [29,68]. These form factors are physical observables when $q^2 \to 0$, and their combinations define the well known electric charge (Q), magnetic dipole (μ), electric dipole (d) and anapole (a) moments.

However, the electromagnetic properties of the neutralino (which is a Majorana particle) are described by a unique form factor, the anapole, $f_A(q^2)$. This is a consequence of CPT-invariance and the C, P, T properties of $\Gamma_\mu(q^2)$ and the interaction Hamiltonian. Thus, the electromagnetic vertex function of the neutralino can be written just as

$$\Gamma_\mu(q^2) = f_A(q^2)(q^2\gamma_\mu - \not{q}q_\mu)\gamma_5. \tag{5}$$

The anapole moment was introduced by Zel'dovich to describe a T-invariant interaction that does not conserve P and C parity [26]. In contrast to the electric and magnetic dipole moments, the anapole moment interacts only with external electromagnetic currents $J_\mu = \partial^\nu F_{\mu\nu}$. In the non-relativistic limit, the interaction energy with an external electromagnetic field takes the form

$$\mathcal{H}_{int} \propto -\mu\left(\sigma \cdot B\right) - d\left(\sigma \cdot E\right) - a\left(\sigma \cdot \bigtriangledown \times B\right), \tag{6}$$

where B and E are the strength of the magnetic and electric fields, and $\vec{\sigma}$ are the Pauli spin matrices.

The anapole moment does not have a simple classical analogue, since $f_A(q^2)$ does not correspond to a multipolar distribution. A more convenient quantity to describe this interaction was proposed by V. M. Dubovik and A. A. Cheshkov [27]: the toroidal dipole moment (TDM), $T(q^2)$. For a comprenhensive review on complete electromagnetic multipole expansions,

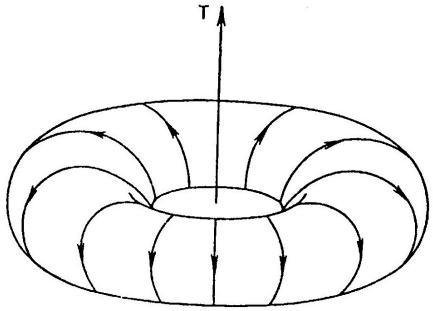


Figure 1: Current configuration with a toroidal dipole moment. The arrows on the torus indicate the direction of the current, and the TDM is directed towards the axis of symmetry of the torus.

including toroidal ones, see [69]. The TDM and the anapole moment coincide in the case of $m_i = m_f$, i.e. the incoming and outgoing particle are the same. This type of static multipole moments does not produce any external fields in vacuum but generate a free-field (gauge invariant) potential [29], which is responsible for topological effects like the Aharonov-Bohm one.

The simplest TDM model (anapole) was given by Zel'dovich as a conventional solenoid rolled up in a torus and with only one poloidal current, see Fig. 1. For such stationary solenoid, without azimuthal components for the current or the electric field, there is only one magnetic azimuthal field different from zero inside the torus.

As mentioned in the introduction, the anapole moment is a very useful quantity in nuclear physics, where it has been widely studied, as well as in astrophysics and engineering. In particle physics it is important in DM detection, since the DM candidates can have couplings to nuclear spins. There are also limits to detection of anapole dark matter in the LHC [43], which exclude it for masses $\lesssim 100$ GeV.

To measure the anapole moment of DM, direct detection is needed, where the resulting cross section from the scattering of the DM particle with a nucleus is measured, and from there the anapole moment or bounds to its value can be extracted. The first such upper bound was calculated in ref. [70], using data from the DAMA/LIBRA collaboration [71] and from the Ge detector

of the CDMS collaboration [72]

$$\sim 4 \times 10^{-2}\text{fm} \tag{7}$$

for a WIMP mass of 100 GeV (3 for the Ge detector and 4 for the NaI one).

There are currently several experiments exploring direct DM detection (for a recent review on indirect and direct DM searches see [73]). The best exclusion bounds for DM at present come from XENON100 [74] and LUX [75]. Although the anapole moment is a very small quantity, it is expected that the improvement in the sensitivity of future direct DM detection experiments will allow to put more stringent bounds on its value. In this respect, knowing precisely the neutron and proton spin contents of relevant nuclei is important for the correct interpretation of the data (see for instance [33–35], and references therein). It is expected that both XENON1T [76] and LUX-ZEPLIN (LZ) [77] will improve by $\sim$ 100 times their measurement of the WIMP-nucleon cross section. In the case of XENON1T the sensitivity is expected to be 2×10^{-47} cm^2 at a WIMP mass of $40 \sim 50$ GeV [76, 78], whereas LZ has a projected sensitivity of 10^{-48} cm^2 for its full 1000 day exposure [77, 79].

4 One-loop calculation

A neutralino is a Majorana particle, and it is necessarily electrically neutral. This fact does not allow for a tree level electromagnetic coupling. Therefore the electromagnetic properties of the Majorana particle –the anapole– arise only via loop contributions. The anapole moment of the neutralino may be defined in the one-loop approximation in the MSSM by the Feynman diagrams shown in Figs. 2 and 3, where f represents the charged fermions of the SM. Taking each fermionic family separately we obtain 96 Feynman diagrams in total, corresponding to self-energies and vertex corrections.

We use *FeynCalc* [80] to calculate the amplitude of these diagrams. Since we are only interested in the terms that contribute to the anapole form factor, we isolate the ones that have the Lorentz structure $\gamma_\mu\gamma_5$. One of the first results we obtain is that the self-energies γH^0, γh^0, γA^0 and γG^0 do not contribute to the calculation at all. If we call Ξ_i the coefficient that multiplies $\gamma_\mu\gamma_5$ for the *ith* diagram, then we have that

$$\sum_i \Xi_i = f_A(q^2)q^2. \tag{8}$$

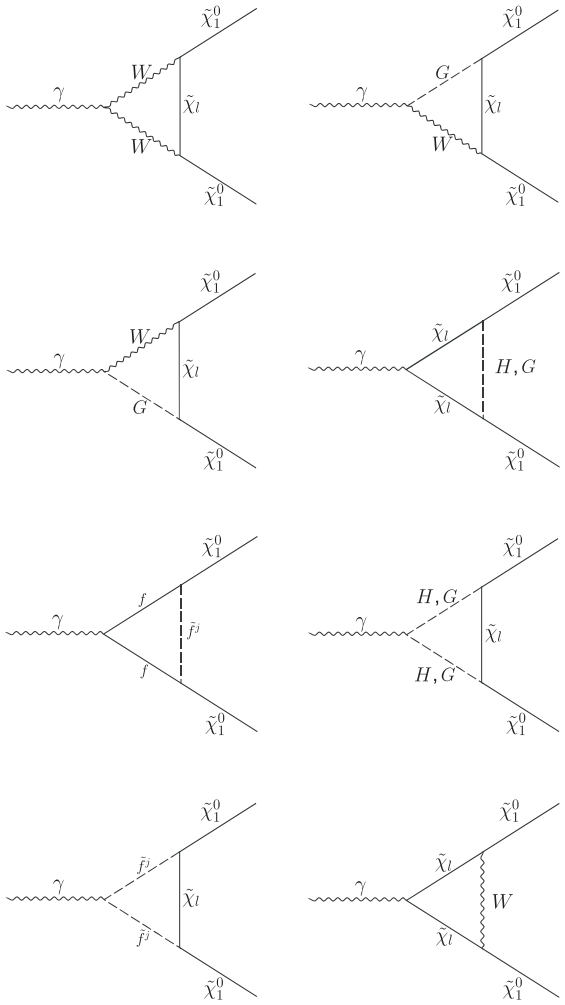


Figure 2: One-loop vertex corrections to the process $\gamma \longrightarrow \chi_1^0 \chi_1^0$.

To obtain the anapole moment $a = f_A(0)$ we use the l'Hopital rule and get

$$a = f_A(0) = \lim_{q^2 \to 0} \frac{\sum_i \Xi_i}{q^2} = \frac{\partial \sum_i \Xi_i}{\partial q^2} \mid_{q^2 \to 0} . \tag{9}$$

Two- and three-point Passarino-Veltman scalar functions arise in the calculation of each diagram. The two-point PV scalar function is defined as

$$B_0(q^2; m_1^2, m_2^2) \equiv \frac{(2\pi\mu)^{4-D}}{i\pi^2} \int \frac{d^D k}{[k^2 - m_1^2][(k+q)^2 - m_2^2]} , \tag{10}$$

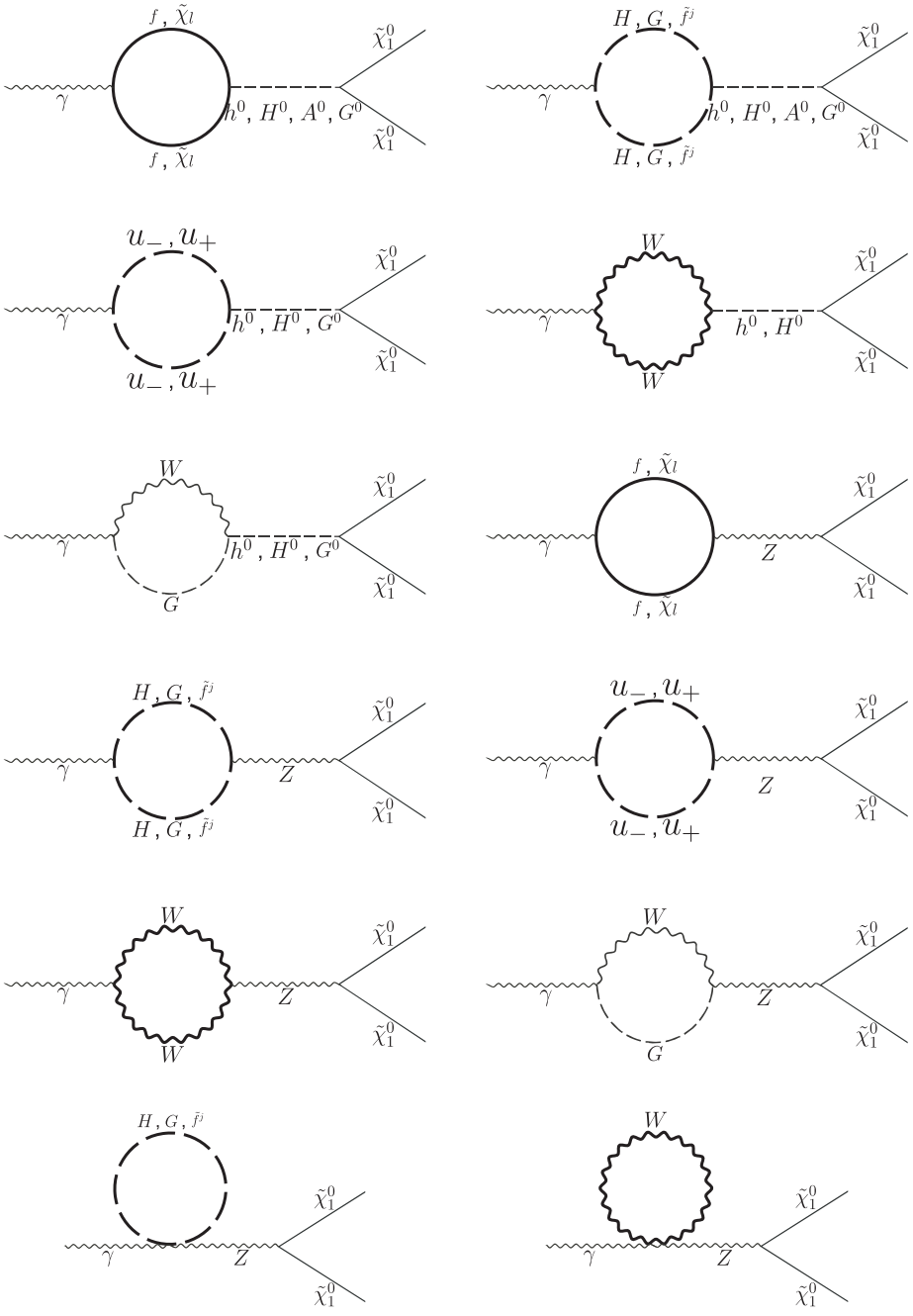


Figure 3: One-loop corrections to the self-energy for the process $\gamma \longrightarrow \chi_1^0 \chi_1^0$.

and the three point PV scalar function is defined as

$$C_0(A,B,C;m_1^2,m_2^2,m_3^2) \equiv$$
$$\frac{(2\pi\mu)^{4-D}}{i\pi^2}\int \frac{d^Dk}{[k^2-m_1^2][(k+p_1)^2-m_2^2][(k+p_2)^2-m_3^2]}\,. \tag{11}$$

where $A = p_1^2, B = (p_1-p_2)^2$ and $C = p_2^2$. The self-energies contain two point Passarino-Veltman scalar functions of the type $B_0\left(q^2,x^2,x^2\right)$ and $B_0\left(0,x^2,x^2\right)$. Likewise, the contributions to the vertex corrections have two and three point scalar functions of the type $B_0\left(q^2,x^2,x^2\right)$, $B_0\left(m^2_{\tilde\chi_1^0},y^2,x^2\right)$ and $C_0\left(q^2,m^2_{\tilde\chi_1^0},m^2_{\tilde\chi_1^0},x^2,x^2,y^2\right)$. In both cases x and y represent the masses of the particles in the loop.

When evaluating (5), derivatives of the Passarino-Veltman functions appear. To evaluate the B_0s, as well as their derivatives, we use *LoopTools* [81]. To evaluate the C_0s and their derivatives we expand them in a power series around $q^2 = 0$. In this way it is possible to find an analytic approximation which coincides with the full expression in the limit $q^2 = 0$, simplifying enormously the calculation (see appendix).

In all regions of parameter space (except for $m_{1/2} \gg m_0$, which is ruled out by cosmological constrains since the LSP is charged) it was observed that the four triangle diagrams involving $\tilde\tau$ in the loop are almost completely dominant. (Fig. 4 shows two of these diagrams. The other two are equal, but with the flow arrows going counterclockwise due to the Majorana nature of the neutralino.) The approximate analytical expressions for the contributions of these diagrams are

$$\Xi_1 \approx \frac{-k}{q^2-4m^2_{\tilde\chi_1^0}}\Big\{(q^2-2m^2_{\tilde\tau}+2m^2_{\tilde\chi_1^0})B_0(q^2,m^2_\tau,m^2_\tau)+2(3m^2_{\tilde\chi_1^0}-m^2_{\tilde\tau})B_0(m^2_{\tilde\chi_1^0},m^2_\tau,m^2_{\tilde\tau}) \tag{12}$$
$$+2\left[(m^2_{\tilde\chi_1^0}-m^2_{\tilde\tau})^2-q^2m^2_{\tilde\chi_1^0}\right]C_0(q^2,m^2_{\tilde\chi_1^0},m^2_{\tilde\chi_1^0},m^2_\tau,m^2_\tau,m^2_{\tilde\tau})-(q^2-4m^2_{\tilde\chi_1^0})\Big\}$$

and

$$\Xi_2 \approx \frac{k}{q^2-4m^2_{\tilde\chi_1^0}}\Big\{(q^2-2m^2_{\tilde\tau}-2m^2_{\tilde\chi_1^0})B_0(q^2,m^2_{\tilde\tau},m^2_{\tilde\tau})+2(m^2_{\tilde\chi_1^0}-m^2_{\tilde\tau})B_0(m^2_{\tilde\chi_1^0},m^2_\tau,m^2_{\tilde\tau}) \tag{13}$$
$$-2(m^2_{\tilde\chi_1^0}-m^2_{\tilde\tau})^2C_0(q^2,m^2_{\tilde\chi_1^0},m^2_{\tilde\chi_1^0},m^2_{\tilde\tau},m^2_{\tilde\tau},m^2_\tau)+(q^2-4m^2_{\tilde\chi_1^0})\Big\}\,,$$

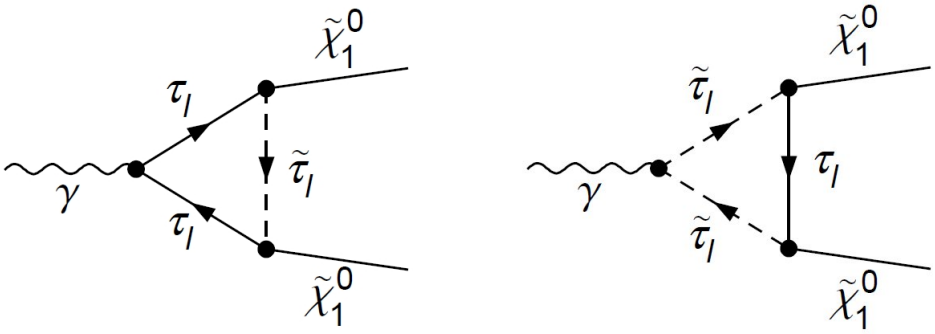


Figure 4: Two of the four dominant Feynman diagrams for the calculation of the anapole moment of the neutralino. The other two are equal but with internal arrows directed counterclockwise.

where k is given by

$$k = \frac{e^3 \left[Z_{1,1}(Z_{2,1} + Z_{1,2}) \cos\theta_W \sin\theta_W + Z_{2,1} Z_{1,2} \cos^2\theta_W - 3 Z_{1,1}^2 \sin^2\theta_W \right] (\cos^2\theta_{\tilde{\tau}} - \sin^2\theta_{\tilde{\tau}})}{128\pi^2 \cos^2\theta_W \sin^2\theta_W (q^2 - 4m_{\tilde{\chi}_1^0}^2)}. \quad (14)$$

These expressions depend on the masses of the particles involved; $Z_{i,j}$, the elements of the neutralino mixing matrix; $\theta_{\tilde{\tau}}$, the $\tilde{\tau}$ mixing angle; as well as the electroweak angle θ_W.

We evaluate the anapole moment within the cMSSM using *Suspect* [82], by fixing the value of A_0, $\tan\beta$ and signμ, and scanning over the other two parameters, m_0 and $m_{1/2}$. We then vary A_0, $\tan\beta$, and signμ, and repeat the procedure. These values we then input into our own code to calculate the anapole moment. This code includes all diagrams contributing to the anapole moment, evaluated using the approximation given in the appendix for the Passarino-Veltman C_0 functions in the limit $q^2 \to 0$. The expressions for each diagram are not shown explicitly in this paper.

We have not considered in our analysis the region where $m_{\tilde{\chi}_1^0}$ and $m_{\tilde{\tau}}$ are degenerate or quasi-degenerate, since this corresponds to a pole in the anapole moment function. Other methods than the one we used here should be employed to analyse this region. Despite the fact that sign$\mu > 0$ may solve the problem of the discrepancy between the measured value of $g-2$ of the muon and the one predicted by the SM, this does not mean negative signμ is ruled out since this problem might be solved through other mechanisms, therefore sign$\mu < 0$ should be also taken into consideration.

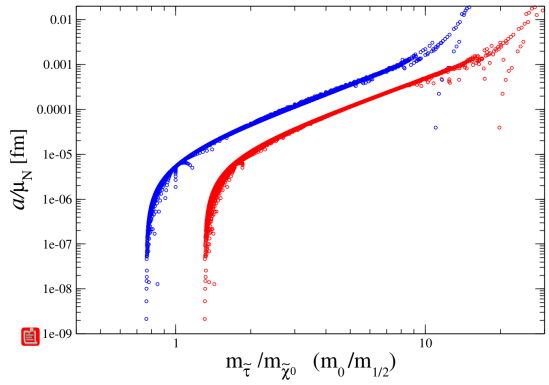


Figure 5: Dependence of the anapole moment (per nuclear magneton) with the $m_{\tilde{\tau}}/m_{\tilde{\chi}_1^0}$ (red) and $m_0/m_{1/2}$ (blue) ratios, for $\tan\beta = 50$. We show only the values where the LSP is the lightest neutralino, and not the stau. The dependence for $\tan\beta = 10$ is similar.

Although the full expression for the anapole moment is a complicated function of the various parameters, it depends mainly on the relative values of $m_{\tilde{\chi}_1^0}$ and $m_{\tilde{\tau}}$, which in turn depend on the ratio of $m_0/m_{1/2}$, as can be seen in Fig. 5. No dependence on A_0 or signμ was found, however, the anapole moment does depend slightly on $\tan\beta$ as can be seen in Fig. 6.

Cosmological and experimental constrains have highly reduced the allowed regions of parameter space of the cMSSM. The most recent of these constrains is the one from the CMS and ATLAS collaborations on the mass of the lightest Higgs boson $m_h = 125.8 \pm 0.6$ GeV [83–86]. This constraint is derived from a combination of 5.1 fb$^{-1}\sqrt{s} = 7$ TeV data and 12.2 fb$^{-1}\sqrt{s} = 8$ TeV data. In our calculation we take this constraint as $m_h = 126 \pm 3$, where the uncertainty comes from a combination of the experimental and theoretical determinations of the Higgs mass.

There is also a new measurement of

$$BR(\tilde{B}_s \to \mu^+\mu^-) = (3.2 \pm 1.5) \times 10^{-9} \tag{15}$$

from the LHCb collaboration, derived from 1fb^{-1} of data at $\sqrt{s} = 7$ TeV collision energy and 1.1fb^{-1} of data at $\sqrt{s} = 8$ TeV collision energy [87]. The excluded region due to this constraint in the cMSSM has already been

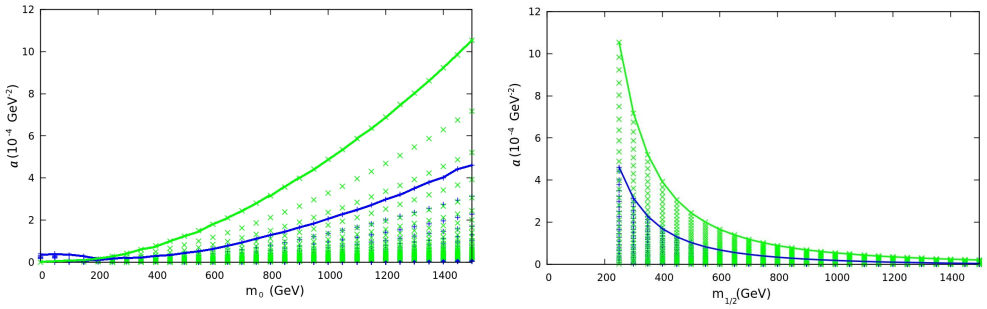


Figure 6: Anapole moment as a function of m_0 and $m_{1/2}$ ($A_0 = 0$ and sign$\mu > 0$ for $\tan\beta = 50$ (blue) and $\tan\beta = 10$ (green). The left panel shows the $m_0 - a$ plane projection while the right panel shows the $m_{1/2} - a$ one. The solid line gives the maximum value of a for that particular $\tan\beta$.

determined in [88]. We also impose the constraint coming from the branching ratio of $b \to s\gamma$, whose value is given by the Heavy Flavour Averaging Group (HFAG) as [89]

$$\mathrm{BR}(b \to s\gamma) = (3.55 \pm 0.24^{+0.09}_{-0.10} \pm 0.03) \times 10^{-4}. \tag{16}$$

This result can be determined directly form Suspect. Moreover, if we assume that neutralinos make up all of the dark matter in the universe, the WMAP 7-year dark matter relic abundance value $\Omega_\chi h^2 = 0.1109 \pm 0.0056$ [45] puts even more strict constraints. We calculated this value using micrOMEGAs [90]. In general, the "surviving" regions have a very small value for the anapole moment of the lightest neutralino (10^{-6}-10^{-7} GeV^{-2}), which is consistent with the results of Ho and Scherrer [22].

In the upper plot of Fig. 7 we show the anapole moment values for different regions of parameter space in $(m_0, m_{1/2})$ planes in the cMSSM for $\tan\beta = 10$. On top and closely around the pink dot-dashed line the stau and neutralino masses are degenerate, and we do not calculate the anapole moment in this region. The plotting program extrapolates between the values on both sides of the line, but there is actually a gap in the data there.

The different phenomenological constraints are shown as follows: the region above the red dashed line is where the Higgs mass is $m_h = 126 \pm 3$ GeV, to the left of the pink dot-dashed line the LSP is charged, under the dotted blue line is the region excluded by the value of $b \to s\gamma$, whereas the region under the dotted green line is excluded because it does not comply with the

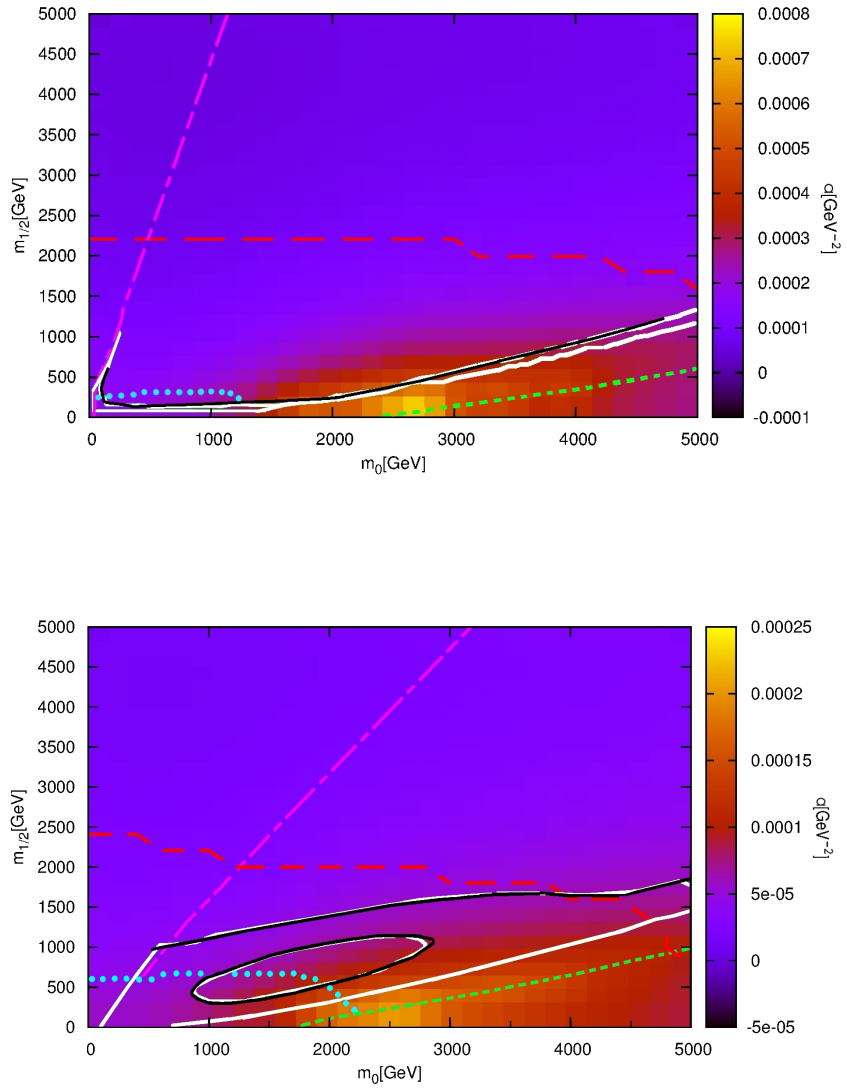


Figure 7: Value of the anapole moment in $(m_0, m_{1/2})$ planes in the cMSSM for $\tan\beta = 10$ (upper plot) and $\tan\beta = 50$ (lower plot), assuming $A_0 = 0$ and $\mu > 0$, see text. The region that complies with all the phenomenological constraints would be to the extreme right of the plots, between the white lines.

requirement of radiative electroweak symmetry breaking. The region where the relic LSP density falls within the range allowed by WMAP is marked with a white line, while a more loose constraint, $\Omega_\chi h^2 < 0.12$, assuming the LSP is not the only component of CDM, is delimited by a white line. The lower plot shows the same regions, but with $\tan\beta = 50$.

In the two graphs we can see that the anapole moment is $\lesssim \mathcal{O}(10^{-4})\text{GeV}^{-2}$ for every region of the space of parameters. That is the case for the bulk (low m_0 and low $m_{1/2}$), already excluded by other constraints. This is also true for the coannihilation region (low m_0 and higher $m_{1/2}$), where the masses of the $\tilde{\chi}_1^0$ and the $\tilde{\tau}$ are almost degenerate. There seems to be a mechanism, which is a function of $m^2_{\tilde{\chi}_1^0} - m^2_{\tilde{\tau}}$, suppressing the contributions from this region. As can be seen from the approximate analytical formulae, there is a dependence on the mass difference between the stau and the neutralino both in the numerator and the denominator. It has to be remembered though that the anapole moment depends on the derivatives of these expressions, which obscures the mechanism at hand. The anapole moment gets relatively large in the focus point region, which corresponds to high m_0 and low $m_{1/2}$, close to the border of viable EWSB (green dotted line). The same behavior is seen for different $\tan\beta$, although the regions might differ in position and size.

In Fig. 8 we show the anapole moment dependence on the neutralino mass, and the exclusion curves of XENON and LUX [23], plus the projected reach of XENON1T and LZ [25]. The regions above the lines of LUX and XENON are the values already excluded by the non-observation of dark matter. The orange points are all the ones where the lightest neutralino is the LSP, the brown ones are the ones that comply with the loose relic density constraint, and the green ones comply with the range of values we took for the Higgs mass. As can be seen from the graphs, the region in parameter space that complies with the Higgs mass constraint is at the border of the reach of LUX and XENON, but within the reach of LZ and XENON1T. For $\tan\beta = 10$ there is practically no region where there is an overlap between the loose relic abundance and Higgs mass constraints, so this region is basically excluded by all three constraints (relic abundance, Higgs mass, and lack of observation of dark matter). For $\tan\beta = 50$ there is a small overlap region between the Higgs mass and relic density constraints. This region lies at the border of the exclusion region of LUX and XENON, but within the projected reach of LZ and XENON1T. If in the future it is possible to measure the anapole moment of a DM candidate, this would give us extra information on the

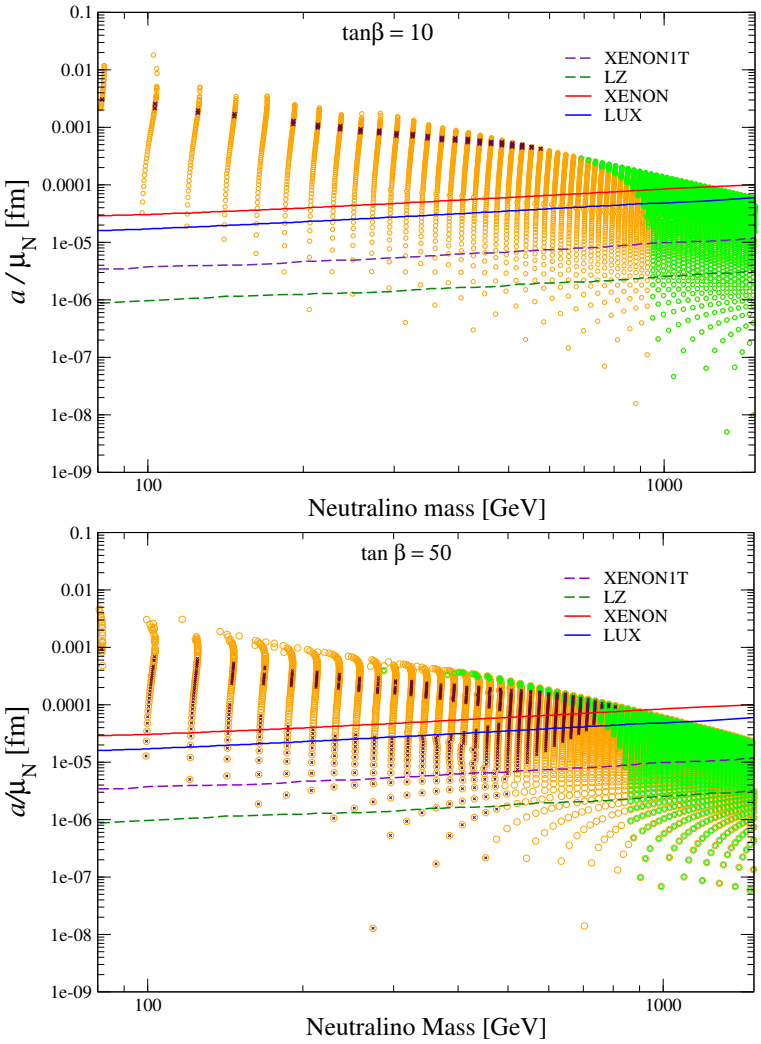


Figure 8: The plots show the dependence on the anapole moment (per nuclear magneton) on the neutralino mass for $\tan\beta = 10$ and 50. The regions above the solid lines correspond to the excluded regions by XENON and LUX, and the ones above the dashed lines correspond to the projected reach of XENON1T and LZ. (See text for an explanation of the different regions.)

allowed parameter space of the cMSSM.

The cMSSM may be too constrained to be realistic, however, using it as a test model, we can see that the anapole moment is indeed different for different regions of parameter space, and is within the reach of the future experiments. Thus, anapole analysis can be used as another criteria to study the parameter space. Although the anapole moment is insensitive to A_0 and signμ, other observables, like the Higgs mass and some decays, are not [51, 54, 56, 58, 66, 91]. This will give different exclusion regions for different values of the cMSSM parameters.

5 Conclusions

We calculated the anapole moment of the lightest neutralino in the framework of the cMSSM. Even though this is perhaps an unrealistically constrained model, it is one of the most studied SUSY models, and therefore it is important to pass it through all possible tests.

We found that the anapole moment of the neutralino is sensitive to m_0, $m_{1/2}$ and $\tan\beta$, but non-dependent on A_0 and signμ. The parameter space we scanned gives rise to an anapole moment consistent with the upper limit obtained by Pospelov and ter Veldhuis [70] for WIMPs interacting with heavy nuclei using data from the CDMS and DAMA experiments. The experimental constraints (Higgs mass, CDM relic density) favour scenarios with large $\tan\beta$. For $\tan\beta = 50$ we found that the anapole moment of the lightest neutralino of the cMSSM has a value $\mathcal{O}(10^{-5} - 10^{-4})$ fm μ_N, which lies at the border of sensitivity of the current experimental searches and within the reach of the future experiments like XENON1T and LZ.

The same kind of calculation can be performed in the context of other more complex models. This could be extremely valuable for discriminating not only between different interesting regions of the cMSSM, but also among different models.

Thus, the anapole analysis could be useful to study the allowed parameter space of the cMSSM and other SUSY models.

Acknowledgements

We acknowledge very useful discussions with S. Heinemeyer, E. Ley Koo, and A. Mondragón, and invaluable technical help from T. Bernal, C. Espinoza, and L. Nellen. We also thank the referee for very useful suggestions and comments that improved the paper.
This work was partially supported by UNAM grants PAPIIT IN113412 and IN111115, and Conacyt grant 132059.

Appendix: Scalar Three-point Function

In this appendix, we analyse the Passarino-Veltman scalar three-point function $C_0(q^2, x^2, x^2, z^2, z^2, y^2)$ [92, 93] which appears in the TDM calculation. Here q^2 denotes the photon transfered 4-momentum, x is the neutralino mass, and y and z are the masses of the particles running in the loop.

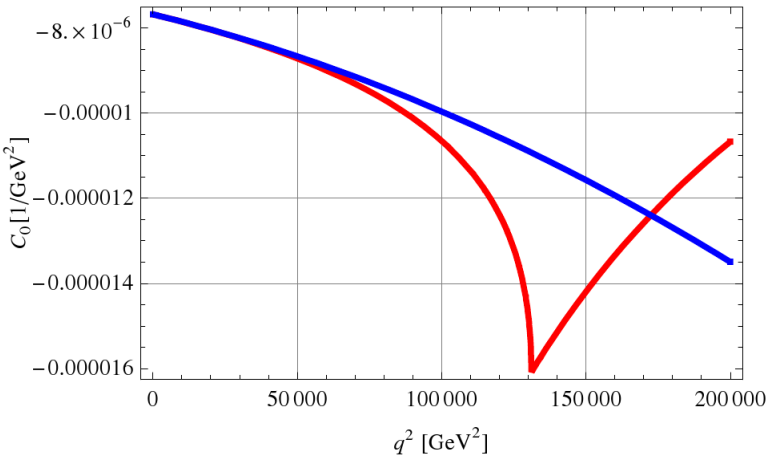


Figure 9: Comparison between numerical (red line) and approximate (blue line) scalar three-point function $C_0(q^2, x^2, x^2, z^2, z^2, y^2)$, with $x = 97.7$ GeV, $y = 415.4$ GeV and $z = 80.43$ GeV. The analytical approximation (blue line) is only valid for $q^2 \to 0$.

The corresponding plot for this C_0 function can be seen in Fig. 9. The red line shows the numerical solution, the blue line line represents the approximate solution, i.e., the Taylor expansion around $q^2 = 0$, which can be written as follows:

$$C_0\left(q^2, x^2, x^2, z^2, z^2, y^2\right) = \alpha_0 + \alpha_1 q^2 + \mathcal{O}(q^4). \tag{17}$$

The coefficients α_i are functions of the masses:

$$\alpha_0 = \frac{\log\left(\frac{y^2}{z^2}\right)}{2x^2} + a\log\omega, \tag{18}$$

$$\alpha_1 = \frac{x^4 - y^2x^2 - 2z^2x^2 + z^4 - y^2z^2}{6x^2z^2(-x+y-z)(x+y-z)(-x+y+z)(x+y+z)} + \frac{\log\left(\frac{y^2}{z^2}\right)}{12x^4} + b\log\omega, \tag{19}$$

where

$$\omega = \frac{\left(ix^2 + iy^2 - iz^2 + \sqrt{-y^4 + 2(x^2+z^2)y^2 - (z^2-x^2)}\right)\left(ix^2 - iy^2 + iz^2 + \sqrt{-y^4 + 2(x^2+z^2)y^2 - (z^2-x^2)}\right)}{\left(-ix^2 + iy^2 - iz^2 + \sqrt{-y^4 + 2(x^2+z^2)y^2 - (z^2-x^2)}\right)\left(-ix^2 - iy^2 + iz^2 + \sqrt{-y^4 + 2(x^2+z^2)y^2 - (z^2-x^2)}\right)}, \tag{20}$$

$$a = \frac{i(x^2+y^2-z^2)}{2x^2\sqrt{-x^4 + 2y^2x^2 + 2z^2x^2 - y^4 - z^4 + 2y^2z^2}} \tag{21}$$

and

$$b = \frac{i(x^2+y^2-z^2)(x^4 - 4y^2x^2 - 2z^2x^2 + y^4 + {}^4 - 2y^2z^2)}{12x^4(-x+y-z)(x+y-z)(-x+y+z)(x+y+z)\sqrt{-x^4 + 2y^2x^2 + 2z^2x^2 - y^4 - z^4 + 2y^2z^2}}. \tag{22}$$

References

[1] A. M. Szelc, Acta Phys.Polon. **B41**, 1417 (2010), arXiv:1010.3918.

[2] R. Schnee, (2011), arXiv:1101.5205.

[3] K. Sigurdson, M. Doran, A. Kurylov, R. R. Caldwell, and M. Kamionkowski, Phys.Rev. **D70**, 083501 (2004), arXiv:astro-ph/0406355.

[4] P. Ciafaloni *et al.*, JCAP **1103**, 019 (2011), arXiv:1009.0224.

[5] P. Ciafaloni and A. Urbano, Phys.Rev. **D82**, 043512 (2010), arXiv:1001.3950.

[6] P. Ciafaloni *et al.*, (2011), arXiv:1104.2996.

[7] N. F. Bell, J. B. Dent, T. D. Jacques, and T. J. Weiler, Phys.Rev. **D83**, 013001 (2011), arXiv:1009.2584.

[8] N. F. Bell, J. B. Dent, T. D. Jacques, and T. J. Weiler, (2011), arXiv:1101.3357.

[9] N. F. Bell *et al.*, (2011), arXiv:1104.3823.

[10] J. B. Dent, R. J. Scherrer, and T. J. Weiler, Phys.Rev. **D78**, 063509 (2008), arXiv:0806.0370.

[11] M. Kachelriess, P. Serpico, and M. Solberg, Phys.Rev. **D80**, 123533 (2009), arXiv:0911.0001.

[12] J. H. Heo, (2009), arXiv:0902.2643.

[13] J. H. Heo, Phys.Lett. **B693**, 255 (2010), arXiv:0901.3815.

[14] S. Liebler and W. Porod, Nucl.Phys. **B849**, 213 (2011), arXiv:1011.6163, * Temporary entry *.

[15] V. Barger, W.-Y. Keung, and D. Marfatia, Phys.Lett. **B696**, 74 (2011), arXiv:1007.4345.

[16] V. Berezinsky, M. Kachelriess, and S. Ostapchenko, Phys.Rev.Lett. **89**, 171802 (2002), arXiv:hep-ph/0205218.

[17] M. Kachelriess and P. Serpico, Phys.Rev. **D76**, 063516 (2007), arXiv:0707.0209.

[18] L. Cabral-Rosetti, M. Mondragon, and E. Reyes Perez, AIP Conf.Proc. **1116**, 447 (2009).

[19] L. Cabral-Rosetti, M. Mondragon, and E. Reyes Perez, J.Phys.Conf.Ser. **315**, 012007 (2011).

[20] L. G. Cabral-Rosetti, M. Mondragon, and E. Reyes-Perez, (2012), arXiv:1206.5052.

[21] L. Cabral-Rosetti, M. Mondragon, and E. Reyes Perez, J.Phys.Conf.Ser. **485**, 012019 (2014).

[22] C. M. Ho and R. J. Scherrer, Phys.Lett. **B722**, 341 (2013), arXiv:1211.0503.

[23] J. Kopp, L. Michaels, and J. Smirnov, JCAP **1404**, 022 (2014), arXiv:1401.6457.

[24] E. Del Nobile, G. B. Gelmini, P. Gondolo, and J.-H. Huh, (2014), arXiv:1401.4508.

[25] A. Ibarra, C. E. Yaguna, and O. Zapata, Phys. Rev. **D93**, 035012 (2016), arXiv:1601.01163.

[26] Y. Zeldovich, Zh. Eksp. Teor. Fiz **33**, 1531 (1957).

[27] V. Dubovik and A. Cheshkov, Sov. J. Particles Nucl. **5**, 318 (1975).

[28] M. Abak and C. Aydin, Europhys. Lett. **4**, 881 (1987).

[29] V. M. Dubovik and V. E. Kuznetsov, Int. J. Mod. Phys. **A13**, 5257 (1998), arXiv:hep-ph/9606258.

[30] E. N. Bukina, V. M. Dubovik, and V. E. Kuznetsov, Phys.Lett. **B435**, 134 (1998), arXiv:hep-ph/9805491.

[31] B. K. Sahoo, T. Aoki, B. P. Das, and Y. Sakemi, (2015), arXiv:1512.02055.

[32] Y. V. Stadnik and V. V. Flambaum, Phys. Rev. **D89**, 043522 (2014), arXiv:1312.6667.

[33] B. M. Roberts *et al.*, Phys. Rev. **D90**, 096005 (2014), arXiv:1409.2564.

[34] Y. V. Stadnik and V. V. Flambaum, Eur. Phys. J. **C75**, 110 (2015), arXiv:1408.2184.

[35] M. I. Gresham and K. M. Zurek, Phys. Rev. **D89**, 123521 (2014), arXiv:1401.3739.

[36] E. O. Kamenetskii, Europhysics Letters **65**, 269 (2004), arXiv:cond-mat:0305431.

[37] A. E. Miroshnichenko *et al.*, Nature communications **6** (2015).

[38] C. H. Page, American Journal of Physics **39**, 1039 (1971).

[39] J. Corum, IEEE Ant. Prop. Int. Symp. **25**, 832 (1987).

[40] G. N. Afanasiev, Journal of Physics A Mathematical General **23**, 5755 (1990).

[41] G. N. Afanasev and V. M. Dubovik, Sov. J. Part. Nucl. **23**, 552 (1992).

[42] N. J. Carron, American Journal of Physics **63**, 717 (1995).

[43] Y. Gao, C. M. Ho, and R. J. Scherrer, (2013), arXiv:1311.5630.

[44] U. Haisch and F. Kahlhoefer, JCAP **1304**, 050 (2013), arXiv:1302.4454.

[45] D. Larson *et al.*, Astrophys.J.Suppl. **192**, 16 (2011), arXiv:1001.4635.

[46] G. Jungman, M. Kamionkowski, and K. Griest, Phys.Rept. **267**, 195 (1996), arXiv:hep-ph/9506380.

[47] K. A. Olive, p. 797 (2003), arXiv:astro-ph/0301505.

[48] J. L. Feng, Ann.Rev.Astron.Astrophys. **48**, 495 (2010), arXiv:1003.0904.

[49] S. P. Martin, (1997), arXiv:hep-ph/9709356.

[50] I. J. Aitchison, (2005), arXiv:hep-ph/0505105, Notes of Lectures for Graduate Students in Particle Physics Oxford, 2004 and 2005.

[51] L. Roszkowski, E. M. Sessolo, and A. J. Williams, JHEP **08**, 067 (2014), arXiv:1405.4289.

[52] A. Fowlie, Eur. Phys. J. **C74**, 3105 (2014), arXiv:1407.7534.

[53] C. Balazs, A. Buckley, D. Carter, B. Farmer, and M. White, Eur. Phys. J. **C73**, 2563 (2013), arXiv:1205.1568.

[54] C. Strege *et al.*, JCAP **1304**, 013 (2013), arXiv:1212.2636.

[55] M. E. Cabrera, J. A. Casas, and R. R. de Austri, JHEP **07**, 182 (2013), arXiv:1212.4821.

[56] O. Buchmueller *et al.*, Eur. Phys. J. **C72**, 2243 (2012), arXiv:1207.7315.

[57] P. Bechtle *et al.*, How alive is constrained SUSY really?, in *37th International Conference on High Energy Physics (ICHEP 2014) Valencia, Spain, July 2-9, 2014*, 2014, arXiv:1410.6035.

[58] E. A. Bagnaschi *et al.*, Eur. Phys. J. **C75**, 500 (2015), arXiv:1508.01173.

[59] P. Bechtle *et al.*, JHEP **06**, 098 (2012), arXiv:1204.4199.

[60] C. Strege *et al.*, JCAP **1203**, 030 (2012), arXiv:1112.4192.

[61] W. Abdallah and S. Khalil, (2015), arXiv:1509.07031.

[62] M. E. Cabrera-Catalan, S. Ando, C. Weniger, and F. Zandanel, Phys. Rev. **D92**, 035018 (2015), arXiv:1503.00599.

[63] J. Ellis *et al.*, (2015), arXiv:1509.08838.

[64] B. C. Allanach, D. P. George, and B. Gripaios, JHEP **07**, 098 (2013), arXiv:1304.5462.

[65] B. C. Allanach, D. P. George, and B. Nachman, JHEP **02**, 031 (2014), arXiv:1311.3960.

[66] O. Buchmueller *et al.*, Eur. Phys. J. **C74**, 2809 (2014), arXiv:1312.5233.

[67] J. Ellis, Prospects for Supersymmetry at the LHC & Beyond, in *18th International Conference From the Planck Scale to the Electroweak Scale (Planck 2015) Ioannina, Greece, May 25-29, 2015*, 2015, arXiv:1510.06204.

[68] E. N. Bukina, V. M. Dubovik, and V. E. Kuznetsov, JINR-E4-98-95.

[69] A. Gongora and E. Ley-Koo, Rev. Mex. Fis. E **52**, 188 (2006).

[70] M. Pospelov and T. ter Veldhuis, Phys. Lett. **B480**, 181 (2000), arXiv:hep-ph/0003010.

[71] R. Bernabei *et al.*, Phys. Lett. **B389**, 757 (1996).

[72] CDMS, R. Abusaidi *et al.*, Phys. Rev. Lett. **84**, 5699 (2000), arXiv:astro-ph/0002471.

[73] M. Klasen, M. Pohl, and G. Sigl, Prog. Part. Nucl. Phys. **85**, 1 (2015), arXiv:1507.03800.

[74] XENON100, E. Aprile *et al.*, Phys. Rev. Lett. **109**, 181301 (2012), arXiv:1207.5988.

[75] LUX, D. S. Akerib *et al.*, Phys. Rev. Lett. **112**, 091303 (2014), arXiv:1310.8214.

[76] XENON, F. A. Davide, EPJ Web Conf. **95**, 04019 (2015).

[77] LZ, D. S. Akerib *et al.*, (2015), arXiv:1509.02910.

[78] XENON100, G. Kessler, XENON100 and XENON1T Dark Matter Search with Liquid Xenon, in *Proceedings, 20th International Conference on Particles and Nuclei (PANIC 14)*, pp. 357–360, 2014.

[79] LUX, J. E. Y. Dobson, Searching for Dark Matter with the LUX experiment, in *Proceedings, 20th International Conference on Particles and Nuclei (PANIC 14)*, pp. 373–377, 2014.

[80] R. Mertig, M. Bohm, and A. Denner, Comput.Phys.Commun. **64**, 345 (1991).

[81] T. Hahn and M. Perez-Victoria, Comput. Phys. Commun. **118**, 153 (1999), arXiv:hep-ph/9807565.

[82] A. Djouadi, J.-L. Kneur, and G. Moultaka, Comput. Phys. Commun. **176**, 426 (2007), arXiv:hep-ph/0211331.

[83] ATLAS Collaboration, G. Aad *et al.*, Phys.Lett. **B716**, 1 (2012), arXiv:1207.7214.

[84] ATLAS Collaboration, (2013), ATLAS-CONF-2013-014, ATLAS-COM-CONF-2013-025.

[85] CMS Collaboration, S. Chatrchyan *et al.*, Phys.Lett. **B716**, 30 (2012), arXiv:1207.7235.

[86] CMS Collaboration, S. Chatrchyan *et al.*, (2013), arXiv:1303.4571.

[87] CMS and LHCb Collaborations, (2013), `http://cdsweb.cern.ch/record/1374913/files/BPH-11-019-pas.pdf`.

[88] A. Arbey, M. Battaglia, F. Mahmoudi, and D. Martinez Santos, Phys.Rev. **D87**, 035026 (2013), arXiv:1212.4887.

[89] (2012), Heavy Flavour Averaging Group, see: `www.slac.stanford.edu/xorg/hfag/`.

[90] G. Belanger, F. Boudjema, A. Pukhov, and A. Semenov, Comput. Phys. Commun. **176**, 367 (2007), arXiv:hep-ph/0607059.

[91] A. Fowlie *et al.*, Phys. Rev. **D86**, 075010 (2012), arXiv:1206.0264.

[92] L. G. Cabral-Rosetti and M. A. Sanchiz-Lozano, J.Comput.Appl.Math. **115**, 93 (2000), arXiv:hep-ph/9809213.

[93] L. G. Cabral-Rosetti and M. A. Sanchiz-Lozano, J.Phys.Conf.Ser. **37**, 82 (2006), arXiv:hep-ph/0206081.